Single photon sources in 4H-SiC metal-oxide-semiconductor field-effect transistors

Y. Abe, T. Umeda, M. Okamoto, R. Kosugi, S. Harada, M. Haruyama, W. Kada, O. Hanaizumi, S. Onoda, and T. Ohshima

Citation: Appl. Phys. Lett. **112**, 031105 (2018); doi: 10.1063/1.4994241
View online: https://doi.org/10.1063/1.4994241
View Table of Contents: http://aip.scitation.org/toc/apl/112/3
Published by the American Institute of Physics

Single photon sources in 4H-SiC metal-oxide-semiconductor field-effect transistors

Y. Abe,[1] T. Umeda,[1,a)] M. Okamoto,[2] R. Kosugi,[2] S. Harada,[2] M. Haruyama,[3] W. Kada,[3] O. Hanaizumi,[3] S. Onoda,[4] and T. Ohshima[4]
[1]*Institute of Applied Physics, University of Tsukuba, Tsukuba 305-8573, Japan*
[2]*National Institute of Advanced Industrial Science and Technology (AIST), Tsukuba 305-8568, Japan*
[3]*School of Science and Technology, Gunma University, Kiryu 376-0052, Japan*
[4]*National Institutes for Quantum and Radiological Science and Technology (QST), Takasaki 370-1292, Japan*

(Received 5 July 2017; accepted 28 December 2017; published online 17 January 2018)

We present single photon sources (SPSs) embedded in 4H-SiC metal-oxide-semiconductor field-effect transistors (MOSFETs). They are formed in the SiC/SiO_2 interface regions of wet-oxidation C-face 4H-SiC MOSFETs and were not found in other C-face and Si-face MOSFETs. Their bright room-temperature photoluminescence (PL) was observed in the range from 550 to 750 nm and revealed variable multi-peak structures as well as variable peak shifts. We characterized a wide variety of their PL spectra as the inevitable variation of local atomic structures at the interface. Their polarization dependence indicates that they are formed at the SiC side of the interface. We also demonstrate that it is possible to switch on/off the SPSs by a bias voltage of the MOSFET. *Published by AIP Publishing.* https://doi.org/10.1063/1.4994241

A state-of-the-art confocal photoluminescence (PL) microscope makes it possible to observe a single luminescent defect (PL center)[1] and even control its photon state[2] and spin states.[3] This ability has great potential for quantum informatics as well as quantum-sensing techniques with an extremely high sensitivity. In principle, a single PL center can emit a single photon at a single PL event, which turns out to be a solid-state implementation of single photon sources (SPSs).[2] One of the most famous examples of SPSs is a negatively charged nitrogen-vacancy center (NV^-) in diamond, which is an extremely bright and stable PL center operatable at room temperature.[1] Recently, further brighter and room-temperature-operatable SPSs have been found in silicon carbides (SiC). For instance, bright SPSs were easily formed in commercial high-purity semi-insulating (HPSI) 4H-SiC wafers after some treatments.[3–5] Furthermore, it has been demonstrated that bulk defects in 4H-SiC (divacancies[3] and silicon vacancies[6]) are suitable for controlling a single spin in an SPS, similar to the case of the NV^- center. Later, Lohrmann *et al*. found bright SPSs in a 4H-SiC device (p^+–n diode) and demonstrated to control them by electrical currents.[7] Since 4H-SiC templates can realize a variety of device structures such as diodes as well as both bipolar and unipolar transistors, it will be quite possible to combine SPSs with various types of 4H-SiC electronic devices.

In this letter, we report SPSs in the channel region of wet-oxidation C-face 4H-SiC metal-oxide-semiconductor field-effect transistors (MOSFETs). The SPSs were formed with a density of $1 \times 10^7\,cm^{-2}$ in the SiC/SiO_2 interface regions, and they emitted very strong PL at room temperature. Their photon emission was more than twice brighter than the PL from a single NV^- center with our confocal microscope (CFM) setup. On the contrary, we have not found any SPSs in dry-oxidation C-face MOSFETs and two types of the standard Si-face MOSFETs. The present SPSs are characterized by a wide variety of PL spectra, suggesting that they are sensitive to local atomic structures at the interface, like a "sensor" for the interface. We also demonstrate a bias-controlled switching of the SPSs by taking advantage of the MOSFET structure.

We used a home-built confocal PL microscope optimized for detecting a single NV^- center in diamond.[8] The PL was excited by a solid-state 532-nm laser. A confocal beam was detected by either a pair of independent photodiodes or a commercial double-grating PL spectrometer. The former detector was used for conventional X–Y–Z CFM mapping and anti-bunching experiments with a Hanbury-Brown-Twiss interferometer,[3–10] where X and Y represent the coordinate axes along the sample surface, and Z indicates the depth from the sample surface ($Z \approx 0$). In this mode, the laser line and background emissions below 647 nm were cut off by long-pass filters to highlight spots of SPSs. For the PL-spectrometer mode, only a long-pass filter of 561 nm was used. We used a high-NA objective lens in air ($NA = 0.95$). By using our CFM setup, a single NV^- center was detectable as a bright spot with a luminescent intensity of about 80 000 counts-per-sec (80 kcps). All measurements described here were done at room temperature.

The lateral n-channel C-face 4H-SiC MOSFETs (gate length/width = 100/150 μm) that we examined were prepared on a 5-μm-thick epitaxial layer of a 4°-off 4H-SiC(000) wafer.[11] The whole image of the MOSFET is shown in Fig. 1(a). The channel region (p^--type) was formed by the epitaxial layer with [Al] $\approx 5 \times 10^{15}\,cm^{-3}$. The source and drain (S/D) regions were formed by phosphorous ion implantation ([P] $\approx 2 \times 10^{20}\,cm^{-3}$) followed by activation annealing at 1620 °C for a few minutes. The 50-nm-thick gate oxide was grown by either wet oxidation at 1000 °C or dry oxidation at 1100–1200 °C. The wet-oxidation C-face MOSFETs were subjected to a post-oxidation anneal (POA) with H_2 gas at 1100 °C, while the dry-oxidation ones were annealed in Ar

a)umeda.takahide.fm@u.tsukuba.ac.jp

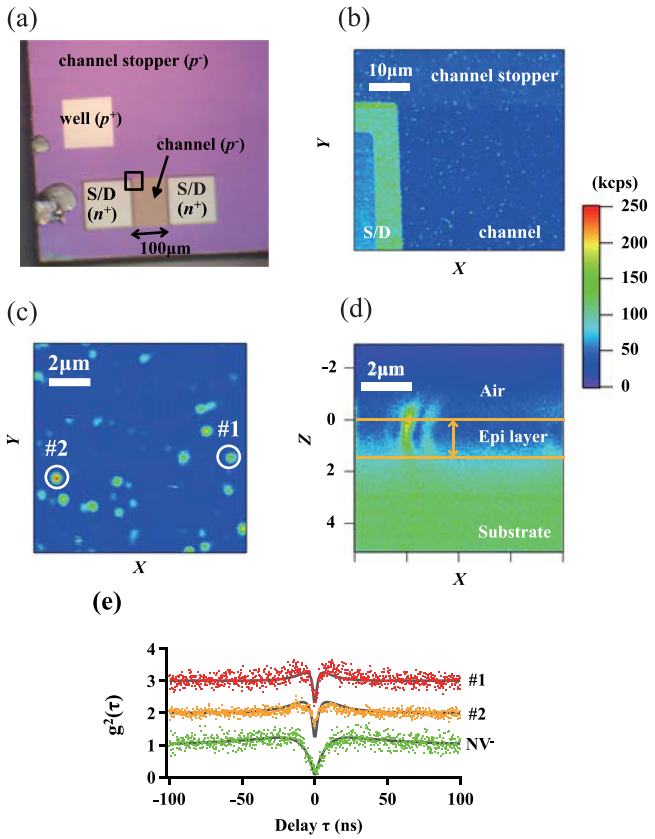

FIG. 1. (a) Optical microscopy image of a wet-oxidation C-face SiC-MOSFET (gate length/width = 100/150 μm) after removing top electrodes. There are four types of regions with different doping concentrations: source/drain (S/D) (n^+), channel (p^-), channel stopper (p), and well (p^+) regions. (b) 50×50-μm^2 CFM image measured for the rectangular region shown in (a). Bright spots in channel and channel-stopper regions arise from SPSs. A bright 5-μm-width periphery of the S/D region was covered by an oxide layer, where PL emission was strongly enhanced. The same periphery was also seen in the well region (not shown in the figure). (c) CFM image of SPSs in the channel region. (d) CFM depth profile for the SPSs. A 5-μm-thick epitaxial layer is shown as a darker layer. The SPSs are always located in the SiC/SiO_2 interface region. (e) Anti-bunching experiments on spots #1 and #2 in (c) and on the reference sample (single NV^- center in diamond) after background corrections. Solid lines expressed fitting curves calculated based on the three-level SPS system.[9] Ratios of (Signal)/(Signal + Background)[10] were 0.88 for spot #1 and 0.92 for spot #2.

ambient at the same temperature and for the same period to ensure that the two C-face MOSFETs had the same thermal history. The p^+-well region was formed by a heavy Al ion implantation ([Al] $\approx 1 \times 10^{20}\,cm^{-3}$). Also, the channel-stopper region (p-type) was prepared by moderate Al implantation ([Al] $\approx 1 \times 10^{18}\,cm^{-3}$) and was covered by a 0.5–μm-thick deposited SiO_2 layer. We also prepared the standard Si-face 4H-SiC MOSFETs by either dry oxidation or dry oxidation + NO POA nitridation for a comparative study between C-face and Si-face MOSFETs. The maximum values of the field-effect mobility (μ_{FE}) were $90\,cm^2 \cdot V^{-1} \cdot s^{-1}$ for the wet-oxidation C-face MOSFETs, $\approx 0\,cm^2 \cdot V^{-1} \cdot s^{-1}$ for the dry-oxidation C-face MOSFETs (no channel currents were activated), $2\,cm^2 \cdot V^{-1} \cdot s^{-1}$ for the dry-oxidation Si-face MOSFETs, and $20\,cm^2 \cdot V^{-1} \cdot s^{-1}$ for the nitrided Si-face MOSFETs.[11]

Before the CFM measurements, the top metal electrodes were removed by wet etching, while we kept the SiO_2 layers as they were. When we removed the SiO_2 layers, the SPSs vanished or their luminescence became unstable. This behavior was consistent with a previous report that an oxide layer was necessary to stabilize SPSs in oxidized HPSI 4H-SiC wafers.[5] Therefore, we believed that the SPSs were confined to the SiC/SiO_2 interface regions, similar to the case of the Lohrmann's study.[5] However, we emphasize that our MOSFETs revealed a different type of SPS, as shown later.

We have confirmed the presence of SPSs *only* in wet-oxidation C-face 4H-SiC MOSFETs (Fig. 1). In Fig. 1(a), the S/D and well regions reveal bare SiC surfaces, while the channel and channel-stopper regions were covered by either a thin (52 nm) or thick (0.5 μm) SiO_2 layer, respectively. The rectangular region in (a) was scanned by CFM, which is shown in Fig. 1(b). The S/D regions (and also the well region) were overall bright; hence, the recognition of SPSs was hardly possible there. On the contrary, the channel and channel-stopper regions showed much lower background emissions (~20 kcps) as well as many isolated bright spots arising from SPSs. Figure 1(c) focuses on SPSs in the channel region. Their luminescent intensities are found to be ~160 kcps for normal spots (spot #1) or ~250 kcps for brighter spots (spot #2), which is at least twice larger than the 80 kcps of a single NV^- center in our setup. The SPSs were formed in the SiC/SiO_2 interface region ($Z \approx 0$), as shown by the X–Z image of Fig. 1(d). In this image, a 5–μm-thick epitaxial layer is visible as a darker 1.9–μm-thick layer [the optical thickness was calculated by dividing the physical thickness by the reflection index of SiC (2.65)]. The present SPSs seemed to be always located at the top of the epitaxial layer; hence, we believe that they originate from a sort of interface defect in SiC/SiO_2 structures.

To demonstrate the correspondence between the bright spots and SPSs, we performed anti-bunching experiments.[3–10] Figure 1(e) shows the normalized self-correlation function $g^{(2)}(\tau)$ measured for the spots #1 and #2 shown in Fig. 1(c), where τ is the delay time between the photon-detection events

TABLE I. Densities of luminescent spots and their luminescent intensities in the channel regions of four types of SiC-MOSFETs. Note that luminescent intensities shown here include background emissions. We compare present data with previous work on oxidized HPSI 4H-SiC wafers.[5]

Sample		Density of luminescent spots ($\times 10^8\,cm^{-2}$)	Luminescent intensity (kcps)
Channel region of 4H-SiC MOSFETs (This work)	C-face wet	0.11 (SPS[a])	160–250
	C-face dry	≥2.9[b,c]	100–120
	Si-face dry	≥1.2[b]	~100
	Si-face nitrided	≥0.7[b]	120–130
Oxidized HPSI 4H-SiC wafers[5]	C-face dry	~8[d]	…
	Si-face dry	~0.8[d] (SPS[a])	…

[a]The observed spots arise from SPSs, which have been confirmed by the anti-bunching experiments.
[b]After subtracting the constant background luminescence, we could find a spotty image and estimate the density of luminescent spots.
[c]Because of severe overlaps of the spots, the density of the spots was roughly estimated by assuming that a single spot should have a circular area of 0.196 μm^2.
[d]We estimated the density of SPSs on the Si face using CFM images shown in Fig. 1 of Ref. 5. For the C face, it was reported that the density of SPSs was one order of magnitude higher than that on the Si face.

of two independent photodetectors.[9,10] For both the spots, their $g^{(2)}(\tau)$ curves were well described with a three-level PL system: $g^{(2)}(\tau) = 1 - (1+a)\exp(-|\tau|/\tau_1) + a\cdot\exp(-|\tau|/\tau_2)$.[9] The solid lines in Fig. 1(e) were calculated with $\tau_1 = 2.6$ ns and $\tau_2 = 15.6$ ns for spot #1 and $\tau_1 = 1.8$ ns and $\tau_2 = 9.2$ ns for spot #2. Using the same setup, we also observed $g^{(2)}(\tau)$ of a single NV^- center [see the bottom curve in Fig. 1(e)], revealing longer lifetimes ($\tau_1 = 7.1$ ns and $\tau_2 = 39.5$ ns). The shorter lifetimes of the present SPSs imply a faster recombination of carriers, which may correspond to their higher brightness compared to those of the NV^- center. Similar higher brightness was commonly found in room-temperature SPSs in 4H-SiC, where similar short lifetimes were observed [$\tau_1 = 1.2$ ns,[4] $\tau_1 = 2.4$ ns,[5] and $\tau_1 = 3.3$ ns (Ref. 7)]. The spots observed in the channel-stopper region also revealed the same features as those of the SPSs in the channel region.

The densities of the SPSs were found to be $1–2 \times 10^7\,\mathrm{cm}^{-2}$ in both the channel and channel-stopper regions (see Table I). By contrast, other MOSFETs with C-face dry-oxidation, Si-face dry-oxidation, and Si-face nitridation did not exhibit any SPSs in both the channel and channel-stopper regions. This is a striking contrast with the previous work[5] that not only 4H-SiC Si-face surfaces but also 6H-SiC and 3C-SiC surfaces easily form SPSs on their surfaces after a brief annealing (800 °C for 5 min) in oxygen ambient.

As described in Table I, our Si-face MOSFETs exhibited isolated bright spots (≥100 kcps) of $\sim 1 \times 10^8\,\mathrm{cm}^{-2}$ under a low background emission (≤30 kcps). Even with such a good condition, we could not have found any anti-bunching behaviors in the two Si-face SiC-MOSFETs. The overall results indicate that the formation of the SPSs is highly sensitive to the preparation of the SiC/SiO_2 interfaces and is not so simple and easy as expected previously. We have to mention that atomic structures of our interfaces should be essentially different from those of the previous studies,[5] owing to

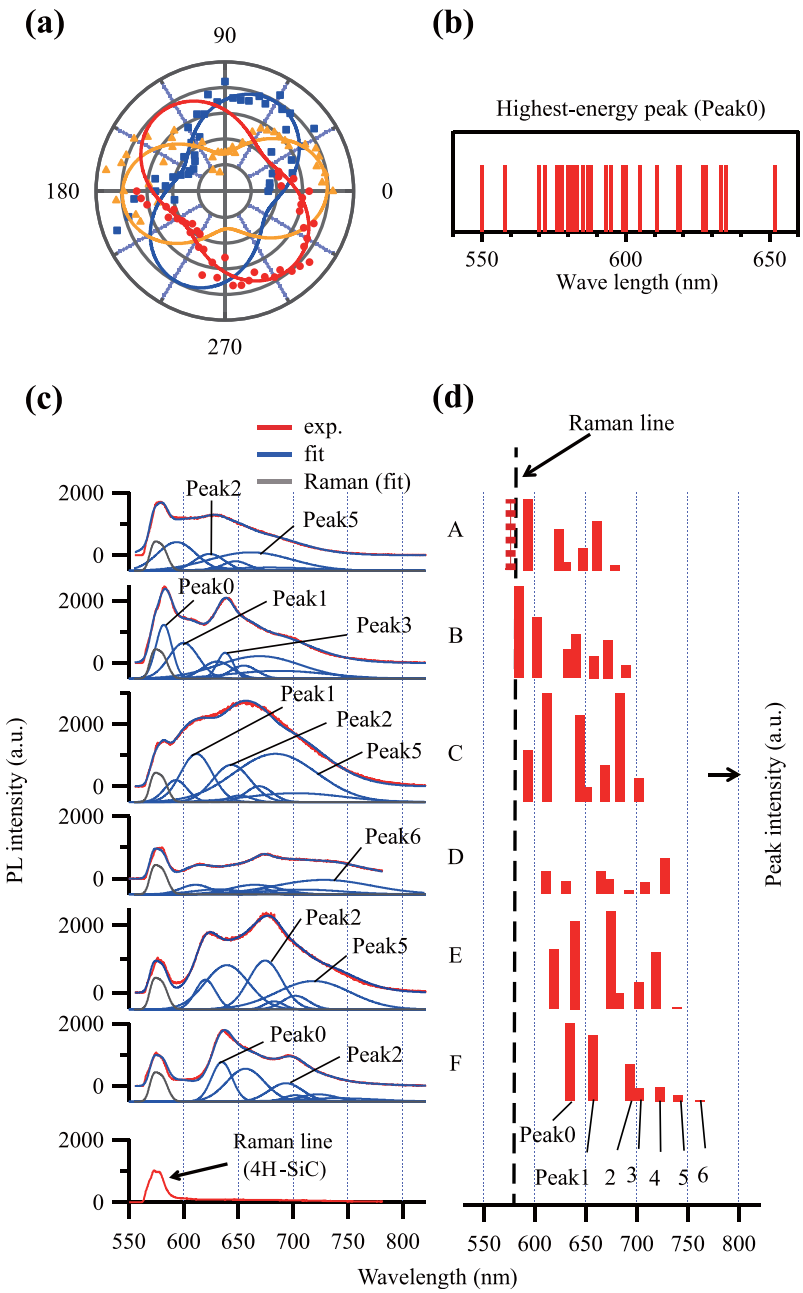

FIG. 2. (a) Polarization dependences of the SPSs. Each emission intensity was normalized to its highest level. The SPSs were classified into three types of orientations in association with a threefold symmetry. (b) Wide variation in the highest-energy peak (Peak0) of the SPSs. Their positions were estimated via fitting analyses described below. (c) PL spectra of individual SPSs ("A" to "F") and fitting results based on our proposed model. All the SPSs revealed similar anti-bunching behaviors as shown in Fig. 1(e). The bottom spectrum was measured at the background position (not on bright spots) and showed the pure secondary Raman line (~580 nm) of 4H-SiC.[15] Each spectrum was normalized such that its secondary Raman line has an equal intensity. PL spectra below 561 nm were not recorded owing to the low-pass filter. (d) Fitting results (peak positions and relative intensities) for the PL spectra "A" to "F." We used a set of the highest-energy peak (Peak0) and six sideband peaks (Peak1 to Peak6) as is summarized in Table II. See also details of the fitting in the text.

TABLE II. A fitting model for PL spectra of the present SPSs, where we assumed a set of the highest-energy peak (Peak0) and six sideband peaks. The position of Peak0 was adjusted for each SPS, while those of the sidebands were fixed to keep energy separations defined in this table. Peak intensities were variable. Full width at half maximum (FWHM) of each peak is given in this table and was allowed to fluctuate by 30% in order to adjust for individual SPS. Possible assignments of the phonon sidebands are also shown in the table.[16,17]

	Peak0	Peak1	Peak2	Peak3	Peak4	Peak5	Peak6
ΔE^a (cm^{-1})	0	515	1330	1510	1920	2240	2630
FWHM (nm)	25	40	40	20	35	75	100
Assignment of local vibration modes	…	SiH_2 Si-O	C-H, C-O	…	…	-C≡C-, Si-H	…

[a]Energy separation in cm^{-1}.

our robust oxidations which accumulate oxidation-induced strain[12] as well as oxidation-induced interstitial atoms[13] in the interface region. Another important difference is the usage of device-grade epitaxial layers, which may prevent the easy formation of SPSs inside MOSFETs.

To examine the origins of the SPSs in wet-oxidation C-face SiC-MOSFETs, we performed polarization and PL experiments on the SPSs. Figure 2(a) shows polarization dependences of the SPSs by rotating a polarization angle of an incident linear-polarized beam. As is seen in the figure, the SPSs clearly show three types of polarization behaviors based on a three-fold symmetry. Since this symmetry coincides with that of the 4H-SiC(000) face, we concluded that the SPSs are formed in the SiC side of the SiC/SiO_2 interfaces. The probability ratio among the above three types appeared to be 0°:120°:240° = 28%:36%:36% with an error of ±9%. Therefore, the SPSs seemed to be uniformly oriented in the 4H-SiC(000) face.

In the next place, the PL spectra of individual SPSs were measured. In Fig. 2(b), positions of the highest-energy PL peak of each SPS are plotted (we call it "Peak0" and its position was estimated via a fitting analysis described below). We found a very wide variation in the peak positions over the energy range of 0.35 eV. Similar wide variations were also seen in zero-phonon lines (ZPL) of other SPSs in SiC [0.17 eV (Ref. 4) and 0.34 eV (Ref. 7)] as well as in diamond [0.23 eV (Ref. 14)]. Since the present SPSs are located in the interface region, it is reasonably expected that their PL spectra varied more widely than the case of SPSs in the bulk region.[4,7,14] For example, we expect that strong local strains at the SiC/SiO_2 interfaces[12] contribute to the wide ZPL variation of the present SPSs. In addition to the peak shifts, the PL spectra exhibited a variety of multi-peak structures [Fig. 2(c)], which is one of the most remarkable differences from the Lohrmann's study.[5] In fact, the previous SPSs exhibited a broad PL signal in the range between 530 and 670 nm.[5] We assumed them to phonon sidebands, because similar multi-peak structures repeatedly appeared in the PL spectra "B" to "F" in Fig. 2(c).

We tried to fit all PL spectra simultaneously by assuming the following model. (i) The highest-energy peaks (presumably ZPLs) are shifted as mentioned in Fig. 2(b). (ii) Multiple phonon sidebands are included, and their intensities are allowed to vary from one SPS to another depending on each local environment. We chose six sideband peaks as indicated by "Peak1" to "Peak6" in Fig. 2(c) and Table II. We should emphasize that the present model is not proven as a unique solution; however, all the PL spectra were successfully fitted, as shown in Fig. 2(c). Figure 2(d) summarizes the fitted positions and intensities of Peak0 and six sideband

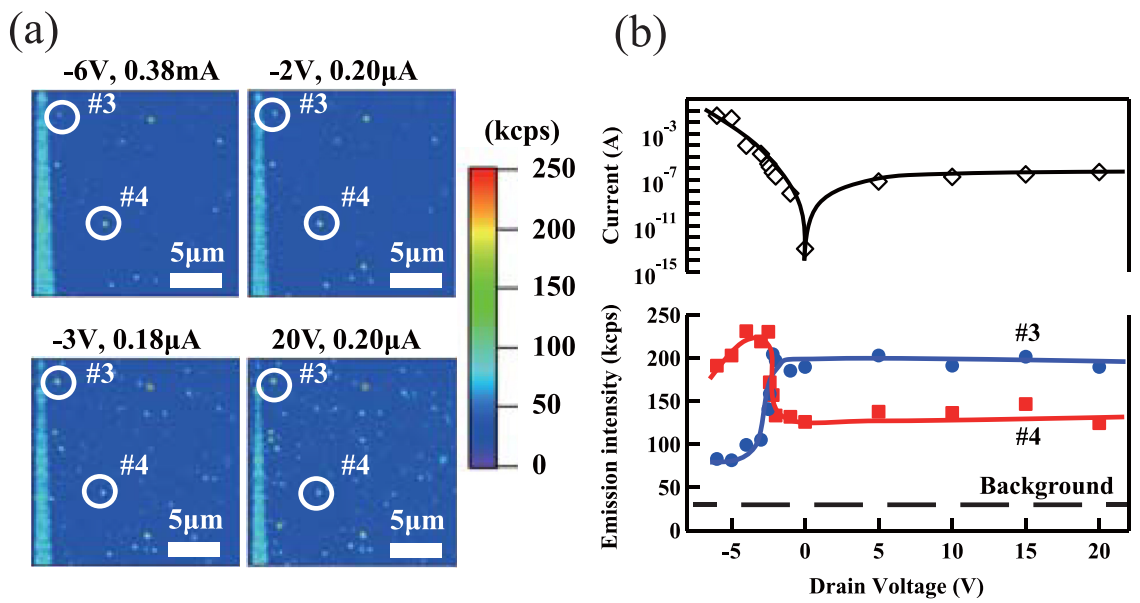

FIG. 3. A bias control of the SPSs in the wet-oxidation C-face 4H-SiC MOSFET. (a) CFM images of an n^+-drain/p-channel-stopper junction of the MOSFET under applying drain biases. A bright region in the left edge is an electrode of the drain. The well contact was set to 0 V, and the source and gate contacts were opened. (b) PL intensities of spots #3 and #4 as a function of the drain bias. The upper figure shows the junction currents.

peaks. Among the six sidebands, the major ones (Peak1, Peak2, and Peak5) are assignable to the local vibration modes of possible interfacial structures such as Si-O, Si-H_2, C-H, or C-O (see Table II). We speculate that the peak intensities reflect on local bonding structures at the interface, and hence, the present SPSs may be usable as a sensor for visualizing local interface structures. We also mention that judging from their PL spectra, if we use an optimal long-pass filter instead of the 647-nm filter used in this study, the luminescent intensities of the present SPSs will be largely enhanced.

Finally, a bias control of the SPSs is examined by utilizing the SPSs in the channel-stopper region of a wet-oxidation C-face MOSFET. Figure 3(a) shows a series of CFM images of an n^+-drain/p-channel-stopper junction, where the n^+-drain region (the left edge) was covered by an Al electrode. We applied a drain bias to the electrode both negatively (the n^+–p junction was forward-biased) and positively (the junction was reversely biased). As is seen in the 20×20–μm^2 images, many SPSs in the channel-stopper region responded to the applied biases. We observed reversible switching behaviors of the SPSs with opposite directions (e.g., spots #3 and #4) in the narrow bias range from -2 V to -3 V, as shown in Fig. 3(b). Further increasing a negative bias generated much larger currents [Fig. 3(b)], but no significant changes were observed for these SPSs. Also positive biases had no impacts on them, although the magnitude of the currents became close to that at -2 V. These observations demonstrate the ability to control the present SPSs by a bias voltage, although the mechanism of the bias control as well as their origins remains future issues to be solved.

In summary, we have found the interfacial SPSs in the channel and channel-stopper regions of wet-oxidation C-face 4H-SiC MOSFETs. These SPSs were much brighter (160 to 250 kcps) than a single NV^- center (80 kcps) in diamond with our CFM setup. The formation of the present SPSs was strongly affected by the oxidation processes, suggesting that they originate from interface defects. In fact, their PL spectra varied widely from one SPS to another, probably depending on the fluctuation of local atomic structures at the interface. This feature is useful for proving the local interface structures around SPSs. Since the present SPSs were sufficiently bright and stable at room temperature and were controllable via bias voltages of the MOSFET, they have potential as an electrically controlled SPS combined with SiC-MOSFETs.

We thank T. Iwasaki and M. Hatano (Tokyo Institute of Technology) for their fruitful advice on our experiments. This work was partly supported by the JSPS KAKENHI Grant Nos. 26286047 and 17H01056.

[1]A. Gruber, A. Dräbenstedt, C. Tietz, L. Fleury, J. Wrachtrup, and C. von Borczyskowski, Science **276**, 2012 (1997).
[2]C. Kurtsiefer, S. Mayer, P. Zarda, and H. Weinfurter, Phys. Rev. Lett. **85**, 290 (2000).
[3]D. J. Christle, A. L. Falk, P. Andrich, P. V. Klimov, J. Ul Hassan, N. T. Son, E. Janzén, T. Ohshima, and D. D. Awschalom, Nat. Mater. **14**, 160–163 (2015).
[4]S. Castelletto, B. C. Johnson, V. Ivády, N. Stavrias, T. Umeda, A. Gali, and T. Ohshima, Nat. Mater. **13**, 151 (2014).
[5]A. Lohrmann, S. Castelletto, J. R. Klein, T. Ohshima, M. Bosi, M. Negri, D. W. M. Lau, B. C. Gibson, S. Prawer, J. C. McCallum, and B. C. Johnson, Appl. Phys. Lett. **108**, 021107 (2016).
[6]M. Widmann, S.-Y. Lee, T. Rendler, N. Tien Son, H. Fedder, S. Pirk, L.-P. Yang, N. Zhao, S. Yang, I. Booker, A. Denisenko, M. Jamali, S. A. Momenzardeh, I. Gerhardt, T. Ohshima, A. Gali, E. Janzén, and J. Warchtrup, Nat. Mater. **14**, 164 (2015).
[7]A. Lohrmann, N. Iwamoto, Z. Bodrog, S. Castelletto, T. Ohshima, T. Karle, A. Gali, S. Prawer, J. McCallum, and B. C. Johnson, Nat. Commun. **6**, 7783 (2015).
[8]S. Onoda, M. Haruyama, T. Teraji, J. isoya, W. Kada, O. Hanaizumi, and T. Ohshima, Phys. Status Solidi (a) **212**, 2641 (2015).
[9]B. Lienhard, T. Schröder, S. Mouradian, F. Dolde, T. T. Tran, I. Aharonovich, and D. Englund, Optica **3**, 768 (2016).
[10]S. C. Kitson, P. Jonsson, J. G. Rarity, and P. R. Tapster, Phys. Rev. A **58**, 620 (1998).
[11]T. Umeda, M. Okamoto, R. Kosugi, R. Arai, Y. Sato, S. Harada, T. Makino, and T. Ohshima, ECS Trans. **58**, 55 (2013).
[12]X. Li, A. Ermakov, V. Amarasinghe, E. Garfunkel, T. Gustafsson, and L. C. Feldman, Appl. Phys. Lett. **110**, 141604 (2017).
[13]D. Goto and Y. Hijikata, J. Phys. D: Appl. Phys. **49**, 225103 (2016).
[14]N. Mizuochi, T. Makino, H. Kato, D. Takeuchi, M. Ogura, H. Okushi, M. Nothaft, P. Neumann, A. Gali, F. Jelezko, J. Wrachtrup, and S. Yamasaki, Nat. Photonics **6**, 299 (2012).
[15]J. C. Burton, L. Sun, F. H. Long, Z. C. Feng, and I. T. Ferguson, Phys. Rev. B **59**, 7282 (1999).
[16]D. R. Lide, *Handbook of Chemistry and Physics*, 86th ed. (CRC Press, 2005–2006).
[17]C. Tsai, K.-H. Li, D. S. KinoSky, R.-Z. Qian, T.-C. Hsu, J. T. Irby, S. K. Banerjee, A. F. Tasch, and J. M. White, Appl. Phys. Lett. **60**, 1700 (1992).